Significance of epidote in orbicular diorite from the Grenville Front zone, eastern Labrador

J. VICTOR OWEN

Department of Geology, Saint Mary's University, Halifax, Nova Scotia, Canada B3H 3C3

Abstract

Orbicules in diorite from the Grenville Front zone of eastern Labrador are defined by shell structures alternately enriched and depleted in biotite, epidote and magnetite. Hornblende occurs locally in orbicule cores and the matrix, but not in the shells. The shells enclose plagioclase-rich (An_{40-45}), leucodioritic cores containing biotite, epidote, magnetite and/or hornblende-bearing mafic clots. The matrix of the orbicules is mineralogically-similar to the orbicule cores, but is mesocratic, and contains relatively sodic plagioclase and accessory quartz and K-feldspar. In places, hornblende contains quartz oikocrysts, implying the resorption of early-formed clinopyroxene, and is rimmed by biotite and epidote. The latter phases also occur as inclusions in quartz-free hornblende interpreted to have crystallized directly from the magma. Epidote has a pistacite content of 21 to 26 and occurs as (1) tiny, idiomorphic crystals ('epidote I') enclosed by plagioclase or hornblende, and (2) relatively large (to 1 mm) grains with vermicular textures ('epidote II'), particularly where in mutual contact with biotite (or hornblende) and plagioclase. These microstructures suggest that epidote is a magmatic phase which formed by direct crystallization from the magma, and by reaction of previously-formed minerals with the magma.

The following approximate paragenetic sequence has been inferred for orbicule cores and the matrix: clinopyroxene (clinopyroxene resorbed [$\rightarrow$ poikilitic hornblende]), epidote I, Ca–Na plagioclase, biotite, hornblende (biotite and/or hornblende $\pm$ plagioclase resorbed [$\rightarrow$ epidote II]), quartz + K-feldspar. Biotite compositions became progressively more Fe-rich during crystallization ($X_{Mg} \simeq 0.6 \rightarrow 0.4$), and the first-formed plagioclase (inclusions in quartz-free hornblende in orbicule cores) is more calcic (An_{51}) than the last (matrix grains: An_{35}).

The appearance of epidote early in the crystallization history of the diorite testifies to elevated P_{H_2O} and P_{Total} (P_T). The most aluminous hornblende indicates maximum P_T of 5 to 6 kbar. Orbicule shell structures are interpreted to have crystallized from supercooled boundary layers enclosing water-saturated globules within the dioritic magma. Although sufficient to suppress the formation of hornblende in the shell structures, the extent of magma supercooling did not permit the development of comb layering in the orbicules. Supercooling is attributed to an influx into the magma of water from an unidentified source.

KEYWORDS: epidote, diorite, orbicules, Grenville Front, Labrador, Canada.

Introduction

THE origin and significance of orbicular structures in granitoid and gabbroic rocks have long been a contentious petrologic problem. Orbicules typically comprise a massive, central core (or an exotic xenolith) enclosed by alternating mafic and felsic shells. The orbicules generally occur in an igneous-appearing matrix, and are commonly associated with comb textures ('Willow Lake-type layering', Taubeneck and Poldervaart, 1960; Moore and Lockwood, 1973) defined by the orientation of inequant minerals perpendicular to layering.

This paper reports on a recently-discovered occurrence of orbicular diorite from eastern Labrador. This occurrence is unusual since epidote is an essential constituent of the orbicular structures, and is interpreted here as a magmatic phase. The paragenetic sequence of crystallization is inferred from microstructures preserved in the diorite, and a model for the formation of the orbicular structures is proposed.

Mineralogical Magazine, June 1991, Vol. 55, pp. 173–181

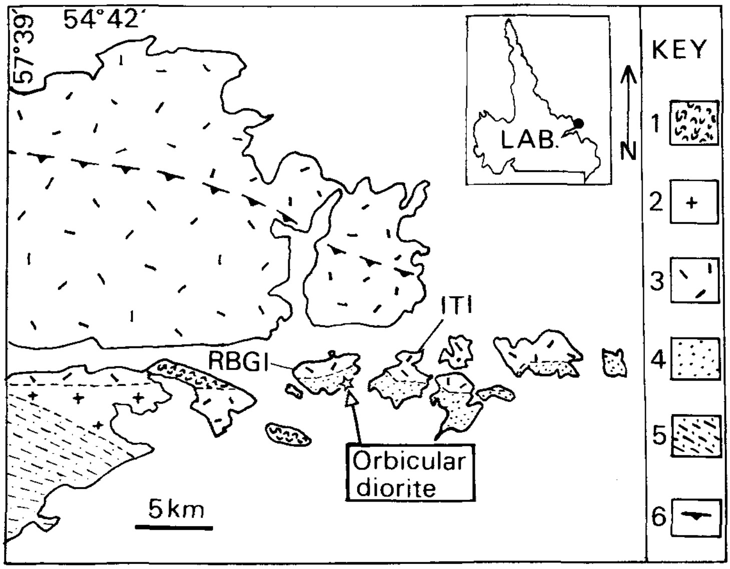

FIG. 1. Simplified geological sketch map of the Grenville Front zone of easternmost Labrador, showing the location of orbicular diorite on Run By Guess Island (RBGI). Key: 1-metagabbro; 2-clinopyroxene-bearing monzonite; 3-granite-granodiorite (ca. 1.7–1.8 Ga); 4-charnockitic gneiss; 5-orthogneiss; 6-Grenville Front (Benedict fault). ITI—Ice Tickle Island.

Field setting and regional geology

Orbicular rocks occur on the southeastern shoreline of Run By Guess Island on the eastern Labrador coast (Fig. 1). Exposure of the diorite is poor owing to vegetation cover, and difficult to sample, so the specimens described here were selected from beach cobbles, which consist almost exclusively of orbicular diorite at the location shown in Fig. 1. At time of field work (1983), outcrop exposure of the diorite was restricted to a few square metres. The maximum on-land areal extent of the orbicular rocks is probably not much more than a few tens of square metres.

The orbicular diorite is enclosed (contacts not seen) by charnockitic gneiss which was partly retrograded during or following regional granitoid plutonism at 1.7 to 1.8 Ga (Owen *et al.*, 1988). The absence of high-grade assemblages in the orbicular diorite and low state of strain of these rocks suggest that they formed after early, high-grade metamorphism in the area. This is supported by the presence of proto-orbicules observed in a narrow dioritic dyke cutting the gneiss on the southwestern shore of Ice Tickle Island, immediately to the east of Run By Guess Island. The age of the orbicular rocks relative to the 1.7–1.8 Ga granitoids, however, is not known.

Petrography

The diorite is a grey, mesocratic, biotite + epidote + hornblende-bearing rock. Accessory phases include quartz, magnetite, microcline, titanite and apatite. The orbicules are spheroidal to ellipsoidal structures showing distinct concentric layering (Fig. 2). Individual orbicules range from 4 to 10 cm in diameter, and have a maximum axial ratio of about 5. In many samples, the orbicules are closely packed, and indent each other. They comprise a medium-grained, plagioclase-rich core (1 to 5 cm in diameter) enclosed by fine-grained, alternating mafic and felsic shells. Xenoliths and comb textures are absent.

Mafic minerals (biotite, hornblende) are inhomogeneously distributed in the core, and in some instances form (together with epidote and magnetite) clots up to 2 cm in diameter. Individual hornblendes may attain 1.5 cm (Fig. 2A). The amphibole is typically mantled in turn by biotite and epidote (Fig. 3A).

Two textural occurrences of epidote are present: (1) tiny ($<$0.2 mm), colourless, (sub)-idiomorphic crystals enclosed by plagioclase and quartz-free hornblende (see below), and (2) relatively large (to 1 mm), colourless to greenish-yellow grains with subidiomorphic shapes (Fig. 3B), and commonly with a vermicular texture

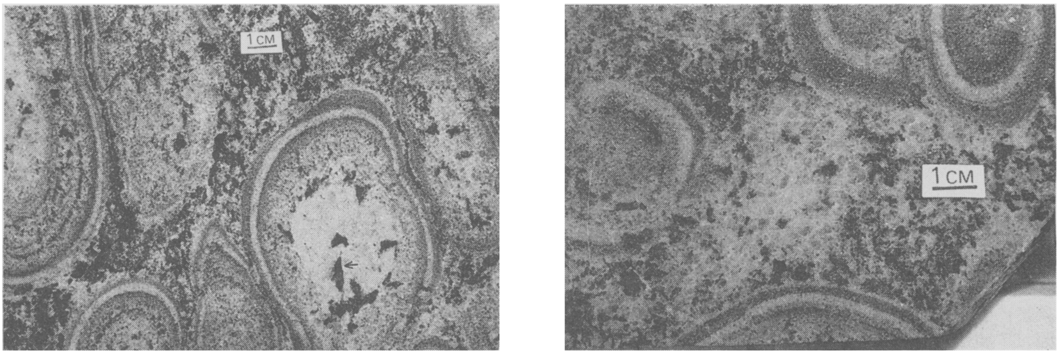

FIG. 2. Photographs of slabbed surface of orbicular diorite from Run By Guess Island, Labrador. A (*left*). Ellipsoidal orbicules showing varying degrees of shell development, the indentation of shell structures by neighbouring orbicules, and the local remobilization of orbicule core material across shells. Note hornblende (see arrow) in the core of some of the orbicules. B (*right*). Ovoid patch of leucocratic material similar to orbicule cores (cf. Fig. 2A) in mesocratic matrix. Note the discordance of shell structures in nearby orbicules (the slab surface here intersects orbicule shell structures rather than their coarser grained core).

(also seen in nearby biotite), particularly where they separate biotite and plagioclase (Fig. 3A) or (to a lesser extent) hornblende and plagioclase. These are referred to as epidote I and II grains respectively. Both occur throughout the diorite, but epidote II is concentrated in the orbicule cores and the matrix.

The contact of the core with the enclosing shells may be abrupt or transitional. Four to six distinct shells are usually present; the innermost is always more mafic than the core. The mafic shells are enriched in biotite, epidote and magnetite, and tend to be wider (*c*. 1–10 mm) and finer grained (*c*. 0.1 mm) than the felsic shells (width *c*. 1–3 mm; grainsize *c*. 0.2–0.8 mm). The felsic shells contain only accessory quantities of epidote. A narrow (1 mm), discontinuous felsic layer often separates the orbicule from the matrix. In places, the shells are disrupted, so the core of the orbicule coalesces with the matrix (Fig. 2A).

The matrix is medium grained, and is mineralogically-similar to the cores of the orbicules, but has a higher colour index (CI *c*. 30), in places is studded with 1 cm plagioclase megacrysts, and contains accessory quartz and traces of microcline. Ovoid, leucocratic patches resembling the orbicule cores occur locally within the more typical, mesocratic matrix (Fig. 2B); some of these are partly enclosed by incipient shell structures.

Mafic minerals in the matrix occur interstitial to plagioclase, and include biotite and minor blue-

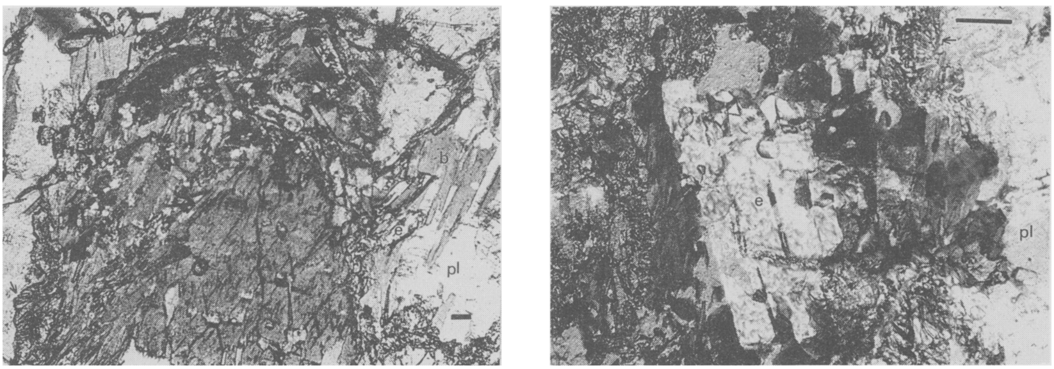

FIG. 3. Photomicrographs of orbicular diorite from Run By Guess Island, Labrador. A (*left*). Mafic clot in orbicule core. Hornblende is enclosed by biotite and epidote, and contains inclusions of both minerals as well as calcic plagioclase (An_{51}). B (*right*). Subidiomorphic epidote II crystal enclosed by biotite in orbicule core. Note the vermicular texture of epidote (see arrow) separating biotite and plagioclase in both photos. Plane polarized light. Bar scale = 0.1 mm; b-biotite, e-epidote, pl-plagioclase. See Table 2 for analyses of the illustrated mafic phases.

green hornblende, which form single crystals or crystal aggregates associated with epidote and magnetite. Some hornblende grains contain abundant quartz oikocrysts, and may therefore represent former clinopyroxene sites. As in the orbicule cores, matrix hornblende is typically enclosed by biotite and epidote.

Mineral chemistry

Samples containing complete orbicules were slabbed, and polished thin sections were prepared in order to provide a complete cross-section across individual orbicule structures and the intervening matrix material. Mineral compositions were determined using a JEOL Superprobe 733 equipped with four wavelength-dispersive spectrometers and one energy-dispersive spectrometer, operated with a beam current of 15 kV at 10 nA. The following geologic standards were employed; jadeite (Al, Si, Na), hornblende (Ca, Ti, Fe, Mg), sanidine (K), Cr metal (Cr), and pyrolusite (Mn). Probe current was measured with a Faraday cage. Data were reduced using a Tracor-Northern ZAF matrix program. Selected mineral analyses and end-member compositions of a hornblende-free orbicule are presented in Table 1. Analyses of mafic clot phase (see Fig. 3) from orbicule cores and the matrix are listed in Table 2. Replicate analyses of the same and nearby grains were undertaken to ensure that those reported here are representative. Core and rim compositions are presented for phases showing analytically-detectable zoning.

Biotite compositions vary according to location in the diorite, and show significant between-sample variations in X_{Mg} [= Mg/(Mg + Fe_T); cf. Tables 1 and 2]. In a sample of a hornblende-free orbicule, biotite within orbicule cores and mafic shells has a slightly more ferroan composition ($X_{Mg} \simeq 0.40$) than biotite in the matrix (X_{Mg} = 0.44–0.47); Table 1). In a sample of a hornblende-bearing orbicule, the most magnesian biotite (X_{Mg} = 0.66; Table 2) occurs as inclusions in quartz-free hornblende in orbicule cores, whereas more ferroan biotite (X_{Mg} = 0.51) mantles the hornblende (Fig. 3A). The magnesian biotite inclusions are interpreted to have crystallized prior to the amphibole, in contrast to the more ferroan biotite.

Plagioclase in all parts of the orbicules is more calcic (An_{37-48}) than plagioclase in the matrix (*c.* An_{35}). Typically, the plagioclase is normally zoned, with rims up to 4 mol.% more sodic than crystal cores. Plagioclase is quite fresh (i.e. shows only incipient saussuritization effects). The most calcic grains (An_{51}) occur as inclusions in quartz-free hornblende in orbicule cores (Fig. 3A; Table 2).

Amphibole compositions were recalculated to 23 oxygen atoms, with all cations except Ca, Na and K being normalized to 13, after which Fe^{3+} was estimated to achieve charge balance. By this procedure, the amphibole is magnesio-hornblende (nomenclature of Leake, 1978). Quartz-free hornblende is more aluminous (*c.* 11 wt.% Al_2O_3, i.e. *c.* 2.0 Al_T per 23 oxygens) than hornblende containing quartz oikocrysts (*c.* 8–9 wt.% Al_2O_3).

Epidote has a pistacite content [= 100*Fe^{3+}/(Fe^{3+} + Al_T)] between 21 and 26. No systematic compositional differences were noted between different textural occurrences of this mineral.

Significance of epidote in the orbicular diorite

Epidote in granitoid rocks is commonly interpreted to be metamorphic; however, experimental data for model granitic, granodioritic, and trondhjemitic systems demonstrate that epidote may crystallize from water-bearing magmas at moderate to high confining pressure (Naney, 1983; Johnston and Wyllie, 1988). Depending on the bulk composition and water content of the magma, and the confining pressure, epidote may crystallize directly from silicate melt, or may form as various mafic phases react with the magma. Epidote formed by the resorption of previously-crystallized phases typically has a vermicular texture (cf. Zen and Hammarstrom, 1984).

Naney's experiments demonstrated that at 8 kbar pressure, epidote is one of the last minerals to crystallize from water-bearing silicious magmas, but that its position in the paragenetic sequence is dependent on the water content of the magma. In the experimental granite system containing 5.8 and 8.0 wt.% water, epidote formed as clinopyroxene was resorbed by the magma, but under water-saturated conditions, epidote preceded both the resorption of clinopyroxene and the crystallization of plagioclase (Naney, 1983; Table 4). Experimental runs on granodioritic compositions showed that igneous epidote was the last phase to crystallize from magma containing between 1 and 4 wt.% water, but during cooling of water-rich magma, epidote crystallized before the resorption of earlier-formed hornblende, and the crystallization of both quartz and K-feldspar. At high confining pressure (15 kbar), epidote is the first phase to crystallize from trondhjemitic melts containing >13% water (Johnston and Wyllie, 1988).

Because Naney's (1983) and Johnston and Wyllie's (1988) experiments were conducted on

Table 1 Composition of selected minerals in a hornblende-free orbicule from the Run By Guess Island orbicular diorite, Labrador

	Orbicule																		Matrix			
	Core					Inner mafic shell			Inner felsic shell		Middle mafic shell			Middle felsic shell	Outer mafic shell			Outer felsic shell				
	Bt*	Pl core	Pl rim	EpII	EpI	Bt	Pl	EpI	Pl core	Pl rim	Bt	Pl core	Pl rim	Pl	Bt	Pl core	Pl rim	Pl	Bt	Pl core	Pl rim	EpII
SiO_2	35.88	57.65	58.82	37.84	38.39	35.78	56.88	38.76	57.40	57.24	35.23	56.49	58.50	57.72	36.12	59.01	59.63	59.97	36.07	60.10	60.08	38.10
TiO_2	3.11	0.00	0.00	0.09	0.04	3.31	0.00	0.13	0.00	0.02	2.99	0.00	0.00	0.00	2.83	0.00	0.00	0.00	3.32	0.00	0.00	0.04
Al_2O_3	17.14	26.86	27.09	25.69	25.62	17.95	27.84	26.10	27.83	27.67	17.17	27.90	27.41	27.58	17.57	26.68	26.10	26.10	16.70	25.44	25.50	25.15
Cr_2O_3	0.06	0.00	0.00	0.00	0.02	0.05	0.00	0.03	0.02	0.00	0.07	0.02	0.03	0.01	0.04	0.03	0.01	0.00	0.05	0.01	0.00	0.04
Fe_2O_3*	nd	nd	nd	11.19	10.89	nd	nd	10.52	nd	nd	nd	nd	nd	nd	nd	nd	nd	nd	nd	nd	nd	11.31
FeO*	20.68	0.08	0.13	nd	nd	20.39	0.08	nd	0.04	0.07	20.95	0.07	0.55	0.00	21.90	0.00	0.19	0.37	19.69	0.05	0.11	nd
MnO	0.26	0.00	0.00	0.22	0.17	0.31	0.00	0.27	0.00	0.00	0.27	0.00	0.00	0.00	0.18	0.00	0.00	0.00	0.29	0.00	0.00	0.39
MgO	8.04	0.00	0.00	0.01	0.00	7.79	0.00	0.00	0.00	0.00	7.84	0.00	0.00	0.00	8.02	0.00	0.01	0.00	8.66	0.00	0.00	0.05
CaO	0.02	8.60	8.15	23.20	23.70	0.07	9.51	23.86	9.48	9.21	0.06	9.51	8.65	8.82	0.01	8.26	7.75	7.38	0.00	7.09	6.90	23.75
Na_2O	0.03	5.77	6.44	0.01	0.01	0.05	5.74	0.00	5.89	6.05	0.09	5.69	6.03	6.40	0.08	6.11	6.70	6.80	0.06	7.34	7.40	0.00
K_2O	9.90	0.11	0.11	0.00	0.00	9.68	0.13	0.00	0.08	0.05	9.43	0.10	0.14	0.02	9.59	0.13	0.10	0.09	9.78	0.22	0.18	0.00
Total	95.1	99.1	100.7	98.3	98.8	95.4	100.2	99.7	100.8	100.3	94.1	99.8	101.3	100.6	96.3	100.2	100.5	100.7	94.6	100.3	100.2	98.8
Endmember compositions																						
X_{Mg}^{Bt}	0.41					0.41					0.40				0.40				0.44			
X_{An}^{Pl}		0.45	0.41				0.47		0.47	0.46		0.48	0.44	0.43		0.42	0.39	0.37		0.34	0.34	
$\%_{Pc}^{Ep}$				21.7	21.3			20.5														22.3

Notes:

* Abbreviations after Kretz (1983). $\%_{Pc}^{Ep}$ = pistacite content of epidote.

* Total Fe as FeO except in epidote (Fe_T as Fe_2O_3)

* nd - not determined

Table 2 Composition of selected minerals comprising mafic clots in orbicule cores and the matrix

	Orbicule cores										Matrix		
	Biotite-rich clot (see Fig. 3B)					Hornblende-rich clot (see Fig. 3A)					Hornblende-rich clot		
	EpII		Bt	EpII	Pl	Hbl*	Bt	Pl	Bt	EpII	Hbl*	Bt	EpII
	1.	2.	3.	4.	5.	6.	7.	8.	9.	10.	11.	12.	13.
SiO_2	37.69	38.06	37.94	37.88	59.65	41.88	37.72	55.27	36.45	37.62	44.62	37.18	37.75
TiO_2	0.15	0.07	2.15	0.10	0.00	1.13	1.85	0.00	2.70	0.11	0.44	1.09	0.05
Al_2O_3	23.99	24.14	15.97	24.57	26.28	11.18	15.41	28.49	17.07	23.85	9.16	16.09	24.90
Cr_2O_3	0.01	0.01	0.11	0.03	0.00	0.05	0.02	0.03	0.03	0.04	0.02	0.05	0.04
Fe_2O_3*	12.34	11.11	nd	12.14	nd	nd	nd	nd	nd	13.22	nd	nd	11.77
FeO*	nd	nd	14.40	nd	0.19	15.72	14.64	0.28	18.44	nd	16.71	16.00	nd
MnO	0.16	0.21	0.28	0.15	0.00	0.30	0.19	0.00	0.15	0.12	0.40	0.23	0.18
MgO	0.00	0.04	14.56	0.05	0.00	11.05	15.72	0.00	10.69	0.03	10.99	13.91	0.00
CaO	23.98	23.93	0.05	23.78	8.54	11.92	0.03	10.68	0.03	24.12	11.91	0.00	23.51
Na_2O	0.00	0.00	0.05	0.03	5.86	1.33	0.09	5.58	0.13	0.02	0.95	0.03	0.00
K_2O	0.00	0.00	9.72	0.00	0.06	1.37	9.29	0.00	9.30	0.00	1.03	9.88	0.00
Total	98.3	97.5	95.2	98.7	100.6	95.9	94.9	100.3	95.0	99.1	96.2	94.5	98.2
Endmember compositions													
X^{Bt}_{Mg}			0.64				0.66		0.51			0.61	
X^{Hbl}_{Mg}						0.56					0.54		
X^{Pl}_{An}					0.44			0.51					
$\%^{Ep}_{Ps}$	24.7	22.7		24.0						26.1			23.2

Notes: 1 & 2 - core and rim (respectively) of subidiomorphic epidote enclosed by biotite
3 - biotite enclosing subidiomorphic epidote
4 - vermicular epidote separating biotite and plagioclase
5 - plagioclase adjacent to vermicular epidote
6 - hornblende core of clot
7 - biotite inclusion in hornblende
8 - plagioclase inclusion in hornblende
9 - biotite mantle on hornblende
10 - vermicular epidote within biotite mantle on hornblende
11 - poikilitic hornblende (contains quartz)
12 - biotite enclosing poikilitic hornblende
13 - vermicular epidote adjacent to biotite

* Total Fe as FeO except in epidote (Fe_T as Fe_2O_3)
* Hornblende formulae from 13 exCNK recalculation scheme (see text):

anal. 6: $(Na^{A}_{.33}\ K_{.27})(Ca_{1.94}\ Na^{M4}_{.07})(Mg_{2.49}\ Fe^{2+}_{1.47}\ {}^{VI}Al_{.34}\ Fe^{3+}_{.53})(Si_{6.34}\ {}^{IV}Al_{1.66})\ O_{22}(OH)_2$

anal. 11: $(Na^{A}_{.20}\ K_{.20})(Ca_{1.92}\ Na^{M4}_{.08})(Mg_{2.46}\ Fe^{2+}_{1.56}\ {}^{VI}Al_{.33}\ Fe^{3+}_{.54})(Si_{6.71}\ Al_{1.29})\ O_{22}(OH)_2$

silica-saturated granitoid rocks, they are not directly pertinent to dioritic rocks (although accessory quartz is present in the diorite described here). They do, however, confirm the importance of P_{H_2O} and P_T in positioning epidote in the paragenetic sequence of water-bearing silicate magmas.

The idiomorphic shape of epidote I, vermicular texture of epidote II, pistacite content of 21–26 for both occurrences of epidote, and the generally unsaussuritized nature of plagioclase support an igneous origin for epidote in the orbicular diorite. Moreover, the concentration of epidote in the mafic shells demonstrates that epidote crystallized during formation of the orbicular structures.

The following microstructural evidence is pertinent to the reconstruction of the paragenetic sequence of the orbicular diorite:

(i) hornblende commonly contains quartz oikocrysts, suggesting the early crystallization and subsequent resorption of clinopyroxene;

(ii) the idiomorphic shape of epidote I crystals and their common occurrence within plagioclase suggest that these grains crystallized prior to the feldspar;

(iii) some hornblende encloses epidote I grains, contains inclusions of biotite and plagioclase with relatively magnesian and calcic compositions (respectively) compared with their counterparts elsewhere in the diorite, and is mantled in turn by biotite and vermicular epidote (epidote II);

(iv) the vermicular appearance of epidote II grains separating biotite and plagioclase or hornblende and plagioclase suggests reaction relations between one or more of these phases and the dioritic magma;

(v) interstitial quartz and microcline occur in accessory quantities in the matrix, particularly near the outer edge of some of the orbicular structures.

These observations suggest the following approximate paragenetic sequence for orbicule cores and the matrix: clinopyroxene, (clinopyroxene resorbed [→ poikilitic hornblende]), epidote I, Ca–Na plagioclase (An_{51}), biotite, hornblende, (hornblende and/or biotite ± plagioclase resorbed [→ epidote II]), quartz + K-feldspar. Biotite and plagioclase crystallized to progressively more ferroan and sodic compositions, respectively. The absence of hornblende in the shells suggests that the shell material crystallized at a lower temperature (e.g. from supercooled magma—see below) than the hornblende liquidus and/or from magma depleted in components essential to nucleating amphibole.

The presence of epidote of apparent magmatic origin implies that the orbicules formed during crystallization of a water-rich magma at moderate to high confining pressure. Confining pressure at the site of crystallization is difficult to estimate, since the Al-in-hornblende geobarometer (Hammarstrom and Zen, 1986; Hollister *et al.*, 1987; Johnson and Rutherford, 1989) is strictly applicable only to granitoid rocks containing primary K-feldspar, which is virtually absent (<1% by volume) in the diorite. Application to the most Al-rich hornblende (i.e. quartz-free grains crystallized directly from the magma; Fig. 3A) yields a pressure of 6.2 kbar using Hammarstrom and Zen's empirical calibration, and a lower pressure (cf. Zen, 1989) of 5.1 kbar using Johnson and Rutherford's experimental calibration. Hollister *et al.*'s (1987) empirical calibration, which incorporates intermediate-pressure data (4–6 kbar) lacking in Hammarstrom and Zen's (1986) method, gives a pressure of 6.6 kbar. These results probably represent maximum values for the confining pressure at the site of crystallization of the diorite, since (1) they are based on the most aluminous igneous hornblende in the rock, and (2) geobarometry of the granulite-grade host rocks, which presumbly provides an upper limit on P_T, indicates values of approximately 4–6 kbar during early (pre-diorite), high-grade metamorphism in the area (Owen *et al.*, 1988).

Discussion

Orbicular structures in granitoid rocks have been variously attributed to magmatic (e.g. Van Diver, 1970; Daugherty and Asquith, 1971; Couturié, 1973; Enz *et al.*, 1979, 1980; McKinney, 1981; Brigham, 1983; Vernon, 1985) or metasomatic (or mixed magmatic/metasomatic) processes (e.g. Leveson, 1963; Simonen, 1966; Thompson and Giles, 1974, 1980; Symes *et al.*, 1987; Yazgan and Mason, 1988). Despite the diversity of ideas forwarded to explain orbicular and related structures, it is generally conceded that P_{H_2O} is an important factor in the formation of these rocks.

The extent of water-saturation controls the liquidus temperature of silicate magma of specified bulk composition. Vernon (1985) postulated that orbicules and comb layering develop where nuclei are destroyed by superheating of initially water-undersaturated magma in response to a sudden influx of water. This permits supercooling of the magma, which forces nucleation on solid objects, thereby accounting for the widely-reported formation of shells structures on xenoliths (e.g. Elliston, 1984). Experimental work on feldspathic melts confirms the importance of supercooling in developing comb textures; the extent of supercooling required to form these structures varies inversely with the viscosity (and therefore with the SiO_2 content) of the magma (Lofgren and Donaldson, 1975). The absence of comb textures and xenolith cores to orbicules in the Run By Guess Island rocks therefore implies a limited degree of supercooling of the relatively non-viscous (compared with granitic systems) dioritic magma.

Mesoscopic features of the orbicules provide clues to their origin. Like many other orbicular rocks, those described here show unequivocal evidence of plasticity prior to final consolidation of the rock: for example, juxtaposed orbicules indent their neighbours (Fig. 2A). Furthermore, the local coalescence of core material with the matrix (Fig. 2A) demonstrates that the core material was not rigid when the enclosing shells formed.

The orbicule cores may represent (1) residual dioritic material formed from inward-crystallizing magma globules; or (2) discrete magma globules upon which the shells subsequently nucleated. In both cases, the orbicule-core magma is interpreted to have been (or become) relatively saturated in water. This would explain the local coalescence of core and matrix material (Fig. 2A), since at a certain critical value (?second boiling; cf. Burnham, 1980), elevated P_{H_2O} would promote remobilization of the residual orbicule core magma so that it disrupts adjacent shells. It also accounts for textural differences between the orbicular cores and the matrix. An elevated water content in the orbicule core magma would promote superheating, thereby destroying (or at least inhibiting the formation of) nuclei, and permitting supercooling. The characteristic occurrence of a few large mafic crystals (or crystal aggregates) in the orbicule cores (Fig. 2A) is attributed to this process.

The progressive decrease in the anorthite content of plagioclase ($An_{48} \rightarrow An_{37}$) in successive shell structures (Table 1) militates against the inward-crystallization of the orbicules. Consequently, the second hypothesis is favoured. In this model, the orbicule core material is interpreted to have formed from water-rich magma globules upon which the shells nucleated. Potentially, this could be evaluated by comparing the concentrations of certain incompatible trace elements in the orbicule cores and the dioritic matrix, since these components should be preferentially partitioned into the globules owing to the disruption of silicate liquid polymer structures by reaction with water (cf. Philpotts, 1990). Furthermore, the hypothesis that the orbicules formed as a result of supercooling potentially may be tested by examining geochemical variations across the orbicules, since their bulk composition would largely be controlled by Soret diffusion processes, assuming that diffusion rates were suitably high.

It is not certain whether the orbicule cores represent pockets of immiscible silicate liquid *sensu stricto*, but this is immaterial to the crystallization model proposed here. Regardless of their origin, the globules appear to have been rheologically distinct from the surrounding dioritic magma. Evidence for the presence within the magma of globules with a high surface tension is provided by ovoid, leucocratic patches in a more mesocratic matrix (Fig. 2B), some of which are partly enclosed by incipient shell structures. Bulk flow of the magma must have been negligible so that the globules remained cohesive, and did not coalesce to form even larger masses.

If the globules became supercooled as a result of their elevated water content, as postulated above, there would be a positive temperature gradient across their boundary with the matrix magma. This apparently promoted the development of an envelope of supercooled boundary layers at the core–matrix interface, which became the site of crystallization of the shell structures. It should be noted that the extent of supercooling at this interface probably exceeded that in the orbicule cores, since the crystallization of hornblende was suppressed in the shell structures (i.e. temperature was less than the hornblende liquidus). In the absence of constrained crystal growth within the orbicules through which latent heat could be extracted by growing crystals (cf. Lofgren and Donaldson, 1975), the cause of the more extensive supercooling postulated for the boundary layers remains problematic. Some globules apparently did not develop supercooled boundary layers; these crystallized as relatively leucocratic patches without well-defined shell structures (Fig. 2B).

The rhythmic mafic and felsic orbicule shells are interpreted to have formed as the supercooled magma alternately became enriched and depleted in the components consumed by the shell crystallizing at any given time, and continued to form until the supercooled conditions required to preserve the boundary layers were no longer prevalent. The degree of undercooling in the boundary layers was insufficient to generate the development of comb layering, probably because of the relatively low viscosity of the intermediate dioritic magma.

The absence of anhydrous mafic phases and the appearance of magmatic epidote early in the paragenetic sequence of the diorite suggest that supercooling resulted from saturation of the magma in water rather than, for example, a rapid decrease in P_T. Although testifying to the elevated water content of the magma, the mineral assemblage does not permit P_{H_2O} to be calculated, so that the possible role of fluctuations in the degree of water-saturation during nucleation of the mafic and felsic shells is difficult to evaluate.

Conclusions

Epidote in orbicular diorite at Run By Guess Island is interpreted as a magmatic phase formed by direct crystallization from the magma (epidote I grains) and by reaction of biotite and/or hornblende (±plagioclase) with the magma (epidote II). The presence of magmatic epidote testifies to a high water content in the magma, and a moderate confining pressure (P_T *c.* 5–6 kbar). If correct, this pressure estimate suggests that primary epidote may crystallize at somewhat lower pressures in water-rich intermediate magmas than in some of their more silicious counterparts.

Local saturation of the magma in water is postulated to have led to the formation of superheated, water-rich globules in the dioritic magma. Superheating destroyed nuclei, or inhibited their formation, and thereby permitted undercooling of the globules, which acted as the nucleus for more highly supercooled boundary layers from which mafic and felsic shell structures crystallized. The temperature of the supercooled boundary layer magma was below the hornblende liquidus. Probably as a result of the relatively non-viscous nature of the dioritic magma (compared with more silicious liquids), however, the extent of supercooling near the core-matrix interface was insufficient to generate comb layering in the orbicules.

Acknowledgements

Field work was supported by Energy, Mines and Resources Canada Research Agreement 241/4/82. Analytical work was funded by a NSERC operating grant. Thanks to J. Dostal and R. F. Symes for reviewing the manuscript, and J. D. Greenough for helpful discussion.

References

Brigham, R. H. (1983) A fluid dynamic appraisal of a model for the origin of comb layering and orbicular structure. *J. Geol.*, **91**, 720–4.

Burnham, C. W. (1980) The importance of volatile constituents. In *The Evolution of the Igneous Rocks. Fiftieth Anniversary Perspectives* (H. S. Yoder, ed.). Princeton Univ. Press, Princeton, N.J. pp. 439–82.

Couturié, J.-P. (1973) Un nouveau gisement de granite orbiculaire dans le Massif Central français: le granite du Signal de Randon (Lozère). *Contrib. Mineral. Petrol.*, **42**, 305–12.

Daugherty, F. W. and Asquith, G. B. (1971) Orbicular rocks from Sandia Mountains, Bernalillo County, New Mexico. *Geol. Soc. Amer., Abstracts with Programs (Rocky Mtns. Section)*, **2**, 375–6.

Elliston, J. N. (1984) Orbicules: An indication of the crystallisation of hydrosilicates, I. *Earth-Sci. Rev.*, **20**, 265–344.

Enz, R. D., Kudo, A. M., and Brookins, D. G. (1979) Igneous origin of orbicular rocks of the Sandia Mountains, New Mexico: Summary. *Geol. Soc. Amer. Bull.*, **90**, 138–40.

——— ——— ——— (1980) Reply to Discussion of 'Igneous origin of orbicular rocks of the Sandia Mountains, New Mexico'. Ibid. **91**, 246–7.

Hammerstrom, J. M. and Zen, E-An (1986) Aluminum in hornblende: An empirical igneous geobarometer. *Amer. Mineral.*, **71**, 1297–313.

Hollister, L. S., Grissom, G. C., Peters, E. K., Stowell, H. H., and Sisson, V. B. (1987) Confirmation of the empirical correlation of Al in hornblende with pressure of solidification of calc-alkaline plutons. Ibid., **72**, 231–9.

Johnson, M. C. and Rutherford, M. J. (1989) Experimental calibration of the aluminum-in-hornblende geobarometer with application to Long Valley caldera (California) volcanic rocks. *Geology*, **17**, 837–41.

Johnston, A. D. and Wyllie, P. J. (1988) Constraints on the origin of Archean trondhjemites based on phase relationships of Nuk gneiss with H_2O at 15 kbar. *Contrib. Mineral. Petrol.*, **100**, 35–46.

Kretz, R. (1983) Symbols for rock-forming minerals. *Amer. Mineral.*, **68**, 277–9.

Leake, B. E. (1978) Nomenclature of amphiboles. *Mineral. Mag.*, **42**, 533–63.

Leveson, D. J. (1963) Orbicular rocks of the Lonesome Mountain area, Beartooth Mountains, Montana and Wyoming. *Geol. Soc. Amer. Bull.*, **74**, 1015–40.

Lofgren, G. E. and Donaldson, C. H. (1975) Curved branching crystals and differentiation in comb-layered rocks. *Contrib. Mineral. Petrol.*, **49**, 309–19.

McKinney, D. B. (1981) Comb layering and orbicular rocks near Fisher Lake, California. *Geol. Soc. Amer., Abstracts with Programs*, **13**, 507.

Moore, J. G. and Lockwood, J. P. (1973) Origin of comb layering and orbicular structure, Sierra Nevada Batholith, California. *Geol. Soc. Amer. Bull.*, **84**, 1–20.

Naney, M. T. (1983) Phase equilibrium of rock-forming ferromagnesian silicates in granitic systems. *Amer. J. Sci.*, **283**, 993–1033.

Owen, J. V., Dallmeyer, R. D., Gower, C. F., and Rivers, T. (1988) Metamorphic conditions and $^{40}Ar/^{39}Ar$ geochronologic contrasts across the Grenville Front zone, coastal Labrador, Canada. *Lithos*, **21**, 13–35.

Philpotts, A. R. (1990) *Principles of Igneous and Metamorphic Petrology*. Prentice Hall, Englewood Cliffs, New Jersey. 498 pp.

Simonen, A. (1966) Orbicular rock in Kuru, Finland. *Comm. Geol. Finlande*, Bull no. 222, 93–107.

Symes, R. F., Bevan, J. C., and Jan, M. Q. (1987) The nature and origin of orbicular rocks from near Deshai, Swat Kohistan, Pakistan. *Mineral. Mag.*, **51**, 635–47.

Taubeneck, W. H. and Poldervaart, A. (1960) Geology of the Elkhorn Mountains, northeastern Oregon: Part 2. Willow Lake intrusion. *Geol. Soc. Amer. Bull.*, **71**, 1295–322.

Thompson, T. B. and Giles, D. L. (1974) Orbicular rocks of the Sandia Mountains, New Mexico. *Geol. Soc. Amer. Bull.*, **85**, 911–6.

——— ——— (1980) Discussion of 'Igneous origin of the orbicular rocks of the Sandia Mountains, New Mexico'. Ibid., **91**, 245–6.

Van Diver, B. B. (1970) Origin of biotite orbicules in 'bullseye granite' of Craftsbury, Vermont. *Amer. J. Sci.*, **268**, 322–40.

Vernon, R. H. (1985) Possible role of superheated magma in the formation of orbicular granitoids. *Geology*, **13**, 843–5.

Yazgan, E. and Mason, R. (1988) Orbicular gabbro from near Baskil, southeastern Turkey. *Mineral. Mag.*, **52**, 161–73.

Zen, E-an (1989) Plumbing the depths of batholiths. *Amer. J. Sci.*, **289**, 1137–57.

——— and Hammerstrom, J. M. (1984) Magmatic epidote and its petrologic significance. *Geology*, **12**, 515–8.

[*Manuscript received 16 March 1990; revised 18 July 1990*]